Biophysical Chemistry, 46 (1993) 77–89
Elsevier Science Publishers B.V., Amsterdam

BIOCHE 01734

Effect of constraints by threonine on proline containing α-helix—A molecular dynamics approach

Shobana S. Vishveshwara and Saraswathi Vishveshwara
Molecular Biophysics Unit, Indian Institute of Science, Bangalore (India)

(Received 28 September 1992; accepted 22 October 1992)

Abstract

Proline plays an important role in the secondary structure of proteins. In the pursuit of understanding its structural role, Proline containing helices with constraints have been studied by employing molecular dynamics (MD) technique. In the present study, the constraint introduced is a threonine residue, whose sidechain has intramolecular hydrogen bond interaction with the backbone oxygen atom. The three systems that have been chosen for characterization are: (1) Ace–$(\mathrm{Ala})_{12}$-Thr–Pro–$(\mathrm{Ala})_{10}$-NHMe, (2) Ace–$(\mathrm{Ala})_{13}$–Pro–Ala–Thr–$(\mathrm{Ala})_8$–NHMe and (3) Ace–$(\mathrm{Ala})_{13}$–Pro–$(\mathrm{Ala})_3$–Thr–$(\mathrm{Ala})_6$–NHMe. The equilibrium structures and structural transitions have been identified by monitoring the backbone dihedral angles, bend related parameters and the hydrogen bond interactions. The MD averages and root mean square (r.m.s.) fluctuations are compared and discussed. Energy minimization has been carried out on selected MD simulated points in order to analyze the characteristics of different conformations.

Keywords: Molecular dynamics; Threonine constraint; Proline containing helices; Structural transitions

1. Introduction

Proline has a special role in the secondary structure of proteins. It has been recognized as a helix breaker and is found to occur in bends and turns [1–6]. Factors that are attributed to these properties of proline are rigidity of the pyrrolidine ring and the lack of hydrogen on the amide nitrogen which disables it from participating in hydrogen bond formation. Its presence in α-helices both in globular proteins and membrane proteins has been noticed [7–10] and studied [7,11–14]. These studies report that a bend of ≃ 23° is introduced in the α-helix.

In nature, these right-handed α-helical segments containing a proline residue are portion of a protein, where the protein environment can influence the conformation of these helices. Moreover, it can depend on other factors such as sequence of the helix, intra- and intermolecular interactions. Therefore, to fully characterize and understand these helices, a systematic study has to be carried out under various conditions. As mentioned above, previous studies were performed on isolated systems with no constraint of the environment. Some studies have also been performed under the influence of its environment [15,16]. However, to understand the properties of

---

Correspondence to: S. Vishveshwara, Molecular Biophysics Unit, Indian Institute of Science, Bangalore (India).

0301-4622/93/$06.00

these helices a systematic study under various constraints are required. In the present study, the proline containing helices with constraints are characterized by molecular dynamics technique. The constraint is introduced by a threonine residue, whose sidechain has intramolecular hydrogen bond interaction with the backbone oxygen atom. Molecular dynamics simulations has been carried out on these systems to identify the equilibrium structures and structural transitions.

2. Methods

In order to explore the conformational properties of proline containing α-helices with constraints introduced in the form of a threonine residue, three systems were chosen. The three systems differ in the position of the threonine residue. They are (1) Ace–$(Ala)_{12}$–Thr–Pro–$(Ala)_{10}$–NHMe, (2) Ace–$(Ala)_{13}$–Pro–Ala–Thr–$(Ala)_8$–NHMe and (3) Ace–$(Ala)_{13}$–Pro–$(Ala)_3$–Thr–$(Ala)_6$–NHMe. In the three systems, the initial conformation includes a hydrogen bond interaction between the O^γ of the threonine sidechain and the i-4th residue (i corresponds the threonine residue). System (1) is a model sequence of helix C of the membrane protein, Bacteriorhodopsin (BR). The starting structure was obtained from the earlier studies on BR [17] where all the residues of helix C except proline and threonine were replaced by alanine. This structure is designated as DP where, the threonine-backbone hydrogen bond is below proline. Systems (2) and (3) were generated from DP by replacing the second and fourth alanine after proline by threonine residues respectively and all other residues except proline were alanine residues. System (2) is designated as AP, where the threonine backbone hydrogen bond is across proline and system (3) is designated as UP, where threonine backbone hydrogen bond is above the proline residue.

Energy minimization studies were carried out using the AMBER [18,19] program adapted to run on an INTEL-860 machine. The partial atomic charges were those suggested by Singh and Kollman and the force field parameters used to evaluate the energy were from Weiner et al. [20,21]. All atoms including the hydrogens were considered in the calculation. A distance-dependent dielectric constant $\epsilon = R_{ij}$ was employed in the evaluation of electrostatic interaction energies. The structures were refined until the r.m.s. gradient of energy was less than 0.001 kcal/mol Å. For the minimization of the three systems, a steepest descent method was used for the first 500 cycles and then a conjugate gradient method was used until convergence.

Molecular dynamics studies were carried out on the three structures, DP, AP and UP using the AMBER–MD module. All bonds involving hydrogens were constrained using the SHAKE algorithm. The simulation was performed in vacuum at 300 K. A time step of 0.001 ps was chosen and the MD run was performed for 200 ps (including an equilibration period of 25 ps) and atomic coordinates were stored at 0.1 ps intervals. Some points from the MD trajectories of DP, AP and UP were also energetically minimized to a convergence of r.m.s. gradient of energy less than 0.001 kcal/mol Å.

The conformational parameters used in the analysis like, the backbone dihedral angles, ϕ, ψ

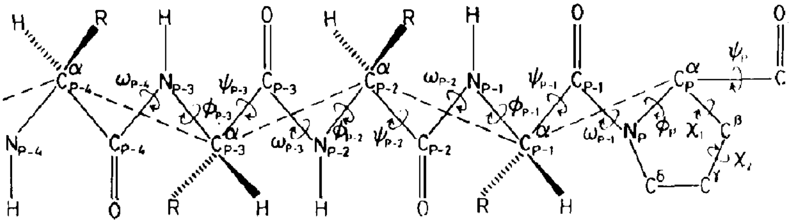

Fig. 1. The conformational parameters of the polypeptide chain containing a proline residue. "R" represents the side chain of the residue. The virtual torsion angle is represented by broken lines.

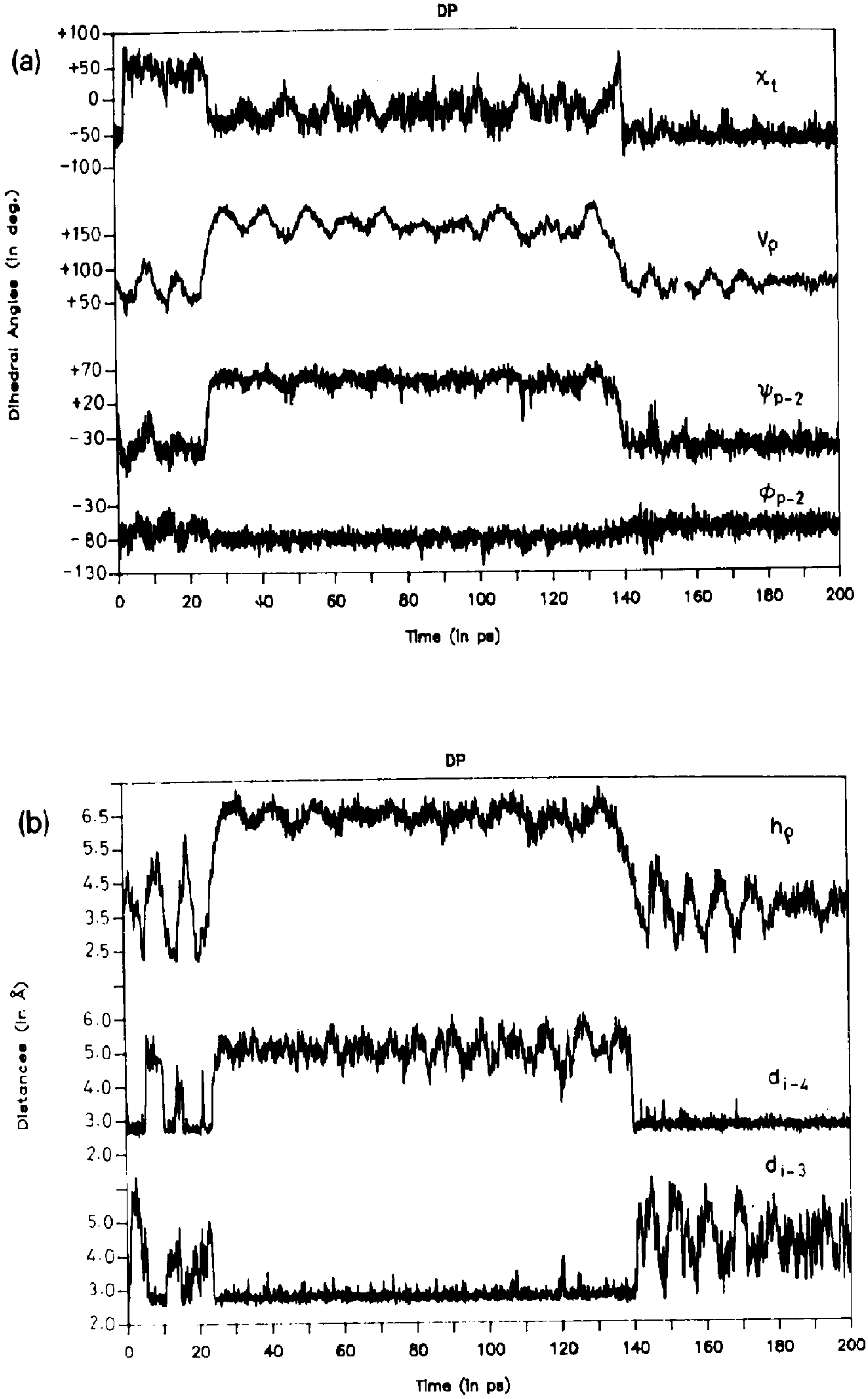

Fig. 2. The MD trajectories of (a) dihedral angles: ϕ_{p-2}, ψ_{p-2}, V_p and χ_t, (b) hydrogen bond distances: d_{i-4}, d_{i-3} and h_p of the simulation with DP as the initial conformation.

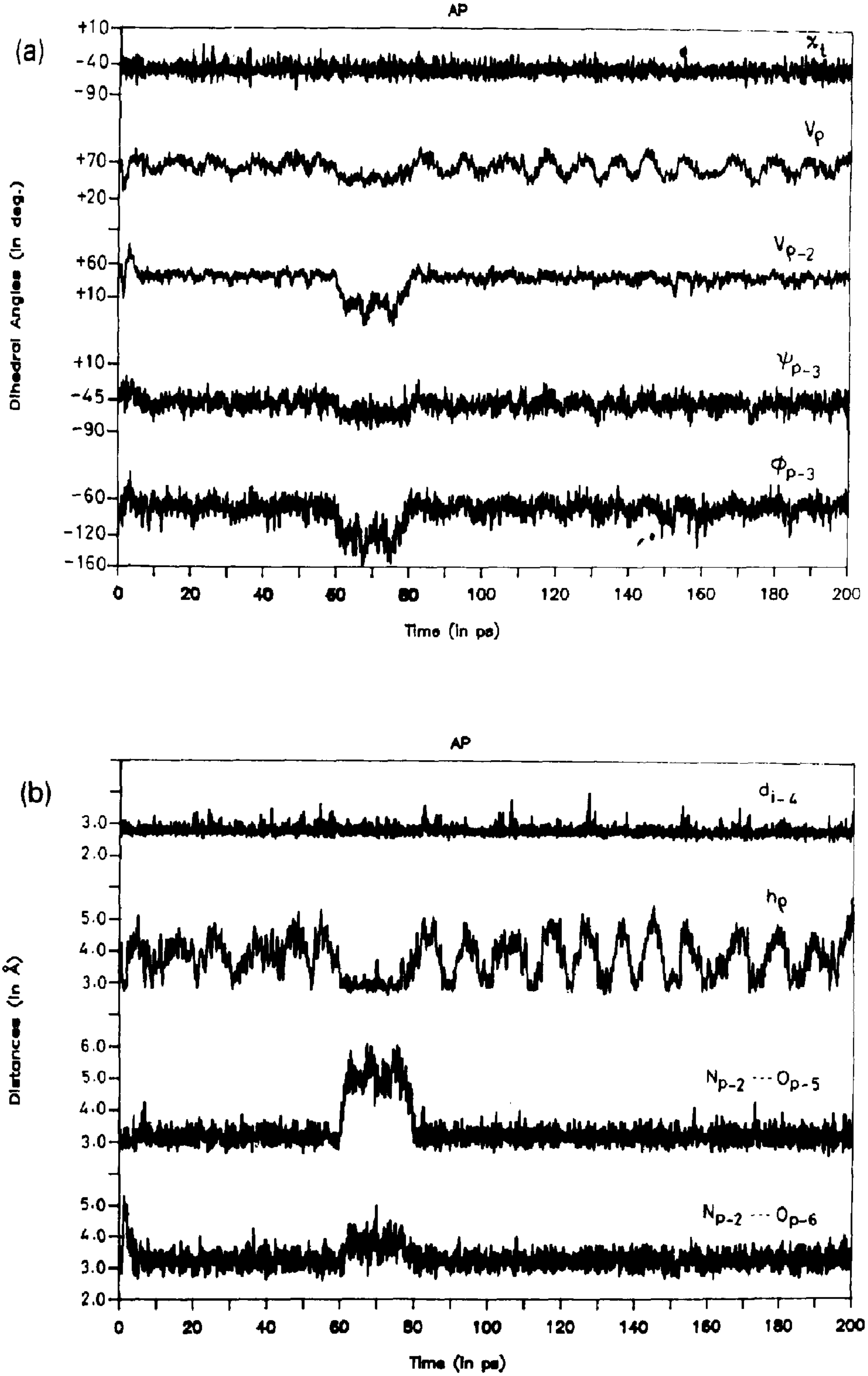

Fig. 3. The MD trajectories of (a) dihedral angles: ϕ_{p-3}, ψ_{p-3}, V_{p-2}, V_p and χ_t, (b) hydrogen bond distances: $N_{p-2}\cdots O_{p-6}$, $N_{p-2}\cdots O_{p-5}$, h_p and d_{i-4} of the simulation with AP as the initial conformation.

and ω and the virtual torsion angles are described in Fig. 1. The bend due to proline was characterized as the kink angle [7,11]. Kink angle is the angle between the two helix axes: one from the N-terminus of the helix to p – 5th residue and th other from the Proline to the C-terminus of the helix. A program was developed in our laboratory to calculate the king angle [13] employing the algorithm suggested by Chou et al. [22]. In order to monitor the α-helical nature of the helices, hydrogen bond interactions were analyzed as the distances between (1) N_i and O_{i-4} ($i \rightarrow i-4$ type) (2) N_i and O_{i-3} ($i \rightarrow i-3$ type) and (3) N_i and O_{i-2} ($i \rightarrow i-2$ type) and their corresponding angles.

3. Results and discussion

Molecular dynamics studies have been carried out on proline containing α-helices with constraints introduced by means of a threonine residue. The results and analysis of MD simulations on DP, AP and UP are presented in this section.

Molecular dynamics simulation on the three systems has provided information on their structural features and structural transitions. The structural features are monitored by the backbone dihedral angles, ϕ and ψ. The values of ϕ, ψ in an ideal α-helix are −57.5°, −47.5° [23] and the averaged values obtained from the crystal structures are −63.8°, −41.0° [24]. The bend related parameters such as virtual torsion angles ($V_p \simeq 50°$ for an ideal α-helix [25]) and kink angle are also monitored during the simulation. In order to investigate the significant deviations from the α-helical parameters, hydrogen bonds of the type $i \rightarrow i-4$, $i \rightarrow i-3$ and $i \rightarrow i-2$ have been analyzed. In an ideal α-helix, the hydrogen bond distances between the N–H of an ith residue and the carbonyl oxygen of the $i-4$th residue is about 2.8–3.0Å and the angle N–H ⋯ O is about 140°–160°. Also, the N ⋯ O distance and the angle N–H ⋯ O in an $i \rightarrow i-3$ type of hydrogen bond is about 3.0–3.5 Å and 110°–130°, respectively, and in an $i \rightarrow i-2$ type the distance is about 3.5–3.7 Å and the angle is about 80°–100°. A good $i \rightarrow i-3$ hydrogen bond is found in a 3_{10}-helix and $i \rightarrow i-2$ type in bent structures [25]. In the present study, ϕ, ψ and ω dihedral angles, virtual torsion angles and the hydrogen bond interactions are used as the parameters to characterize the structural features and transitions in the three systems, DP, AP and UP. Threonine-backbone hydrogen bonds are also monitored during the simulations.

The trajectories of parameters which have changed during MD simulation or deviated from the normal α-helical values in the system DP are given in Figs. 2a and 2b. The starting conformation chosen for simulation is the minimized proline containing α-helix with a kink angle of 29.1° (manuscript in preparation). At the end of the equilibration period, a structural transition occurs and this new conformation is retained up to 140 ps and then reverts back to a form close to its initial conformation. This is clearly evident from the trajectories of ϕ_{p-2}, ψ_{p-2}, V_ρ, χ_t (Fig. 2a), where χ_t is the sidechain dihedral angle of threonine (C^α–C^β–C^γ–O^γ) and $N_{p+1} \cdots O_{p-3}$ (h_ρ) · $O_i^\gamma \cdots O_{i-4}$ (designated as d_{i-4}) and $O_i^\gamma \cdots O_{i-3}$ (designated as d_{i-3}) (Fig. 2b), where i is the threonine residue. For the purpose of analysis, the structure observed up to 140 ps is designated as DP2 and that between 140 ps and 200 ps as DP1. The trajectories of the parameters ϕ_{p-3}, ψ_{p-3}, $V_{\rho-2}$, V_ρ and χ_t of the system AP and the hydrogen bond parameters $N_{p-2} \cdots O_{p-6}$, $N_{p-2} \cdots O_{p-5}$, h_ρ and d_{i-4} are given in Figs. 3a and 3b. The system attains a different conformation designated as AP1 for a brief period of 20 ps between 60 ps and 80 ps. The changed parameters are given in Figs. 3a and 3b. The conformation accessed during the major part of the simulation is designated as AP2. The trajectories related to the system UP are are given in Figs. 4a and 4b. At about the end of the equilibration period, the system takes on a conformation different from its starting structure. This conformation is retained during most of the simulation period and is designated as UP2. For a short period of about 20 ps (between 80 ps and 100 ps), a different conformation designated as UP1 is accessed. The trajectories of the parameters involved in this structural transition are ψ_{p-3}, ψ_{p-2},

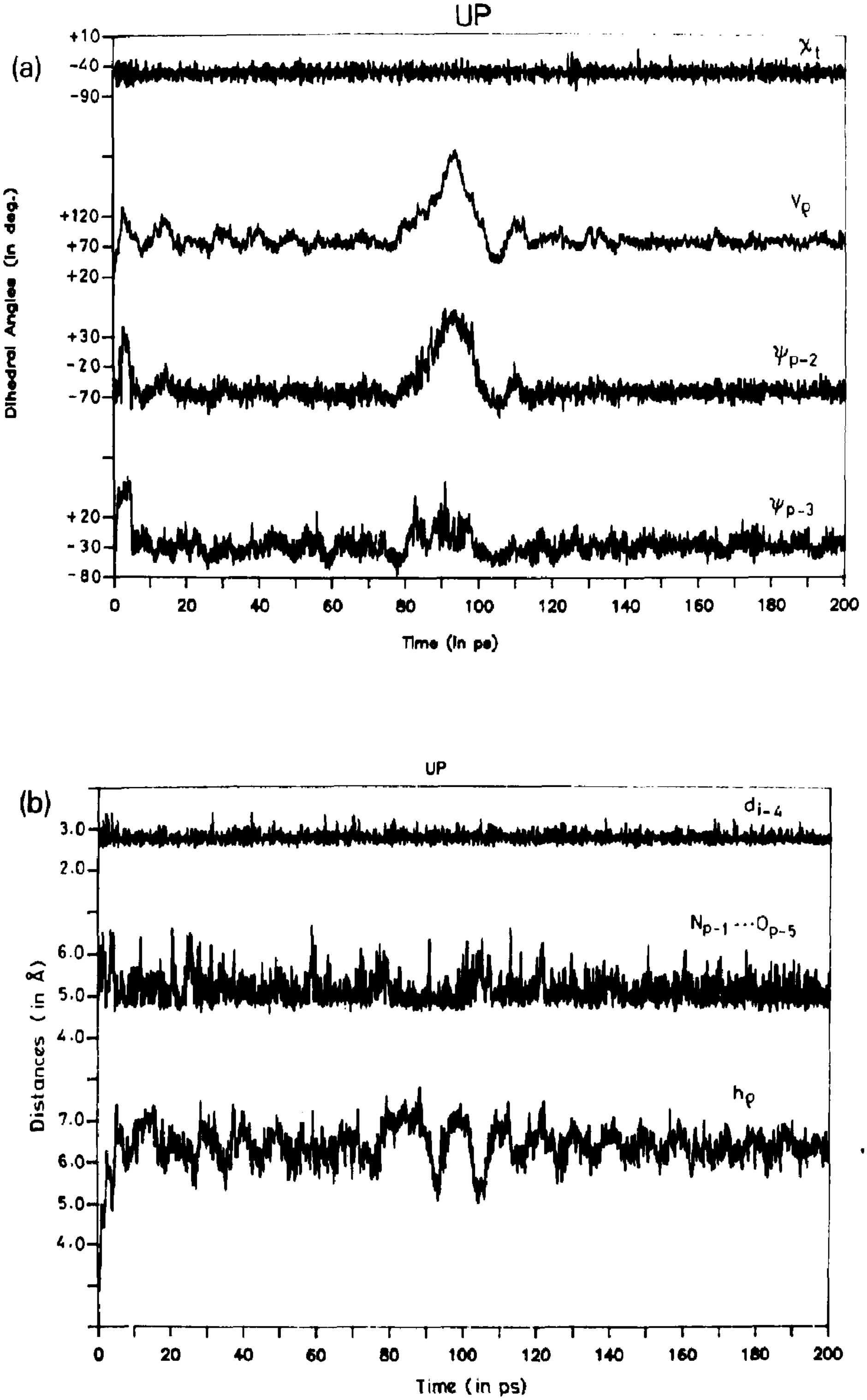

Fig. 4. The MD trajectories of (a) dihedral angles: ψ_{p-3}, ψ_{p-2}, V_p and χ_t (b) hydrogen bond distances: $N_{p-1} \cdots O_{p-5}$, h_p and d_{i-4} of the simulation with UP as the initial conformation.

Table 1

The backbone dihedral angles (in degrees) for the three simulations DP, AP and UP are given. The three entries for every parameter listed are the MD average, the r.m.s. deviation and the value corresponding to the MD minimized structure, respectively

Dihedral angle	DP1	DP2	AP1	AP2	UP1	UP2
ϕ_{p-4}	-57.24	-59.91	-69.68	-58.39	-59.32	-60.48
	(±8.87)	(±9.49)	(±11.01)	(±9.39)	(±9.63)	(±10.20)
	-58.76	-57.88	-70.55	-58.27	-55.06	-54.90
ψ_{p-4}	-44.09	-46.23	-43.50	-39.51	-40.48	-44.55
	(±10.48)	(±9.83)	(±13.51)	(±12.18)	(±11.46)	(±10.03)
	-38.22	-47.50	-46.49	-33.47	-43.45	-44.71
ω_{p-4}	176.73	177.94	-170.59	175.55	176.13	176.86
	(±6.27)	(±7.16)	(±7.06)	(±6.92)	(±6.25)	(±6.76)
	175.23	176.75	-166.06	171.81	177.90	177.31
ϕ_{p-3}	-65.90	-61.04	-116.92	-70.84	-73.05	-66.87
	(±10.77)	(±10.66)	(±7.72)	(±12.32)	(±12.01)	(±10.54)
	-72.71	-58.82	-125.54	-77.57	-74.36	-68.29
ψ_{p-3}	-44.99	-47.77	-60.09	-46.21	-4.26	-26.36
	(±8.97)	(±10.17)	(±10.78)	(±10.40)	(±21.85)	(±12.80)
	-49.19	-50.77	-62.39	-50.56	-2.85	-18.08
ω_{p-3}	-176.81	176.45	-166.33	-175.06	177.05	173.90
	(±7.26)	(±7.82)	(±7.07)	(±8.14)	(±11.72)	(±8.54)
	-174.00	179.56	-162.41	-175.56	-174.65	176.70
ϕ_{p-2}	-65.42	-79.41	-63.05	-65.13	64.80	71.85
	(±10.05)	(±9.36)	(±9.15)	(±11.63)	(±14.52)	(±8.84)
	-61.57	-78.21	-66.79	-56.66	51.47	68.90
ψ_{p-2}	-45.48	+47.64	-48.70	-45.46	11.59	-61.16
	(±10.86)	(±23.24)	(±8.67)	(±10.98)	(±40.17)	(±9.91)
	-49.53	+45.05	-46.29	-46.74	45.35	-65.74
ω_{p-2}	-173.20	-172.13	180.23	-172.79	-178.68	-176.80
	(±6.71)	(±9.06)	(±5.68)	(±7.82)	(±10.83)	(±8.32)
	-173.94	-175.82	179.21	178.15	-173.94	-175.10
ϕ_{p-1}	-43.10	-49.95	-60.01	-50.60	-39.38	-48.25
	(±11.16)	(±9.64)	(±8.29)	(±10.98)	(±17.96)	(±10.98)
	-49.44	-53.38	-63.64	-57.89	-33.77	-52.62
ψ_{p-1}	-61.36	-47.86	-57.46	-50.60	-58.17	-51.13
	(±7.64)	(±8.24)	(±7.91)	(±10.98)	(±9.73)	(±8.85)
	-60.76	-50.34	-52.69	-57.89	-58.72	-46.99
ω_{p-1}	-179.78	176.34	169.13	177.25	179.84	177.16
	(±5.82)	(±6.81)	(±5.55)	(±7.36)	(±6.45)	(±7.27)
	-179.88	177.92	168.40	167.68	-179.76	178.24
ϕ_{p}	-60.09	-53.21	-45.82	-56.33	-58.81	-57.39
	(±7.87)	(±10.08)	(±9.16)	(±10.01)	(±8.86)	(±9.18)
	-61.20	-53.83	-44.86	-43.34	-44.08	-49.35
ψ_{p}	-43.22	-45.00	-51.47	-45.54	-44.08	-46.75
	(±9.14)	(±9.44)	(±10.05)	(±10.12)	(±9.79)	(±9.62)
	-41.04	-48.76	-53.05	-51.71	-42.94	-49.35
ω_{p}	178.91	179.39	179.82	179.23	178.93	178.75
	(±6.75)	(±6.52)	(±8.25)	(±6.43)	(±6.72)	(±6.30)
	178.47	-179.22	179.86	-179.16	-179.88	178.37
ϕ_{p+1}	-60.45	-63.39	-58.02	-59.19	-40.38	-60.91
	(±9.75)	(±9.44)	(±10.95)	(±9.62)	(±19.96)	(±9.52)
	-58.52	-62.80	-57.38	-53.93	-62.70	-58.54
ψ_{p+1}	-48.46	-47.32	-47.00	-46.60	-58.17	-48.86
	(±8.47)	(±8.85)	(±9.04)	(±8.97)	(±9.73)	(±8.55)
	-50.47	-48.65	-48.06	-47.21	-47.37	-49.12
ω_{p+1}	177.01	176.89	177.64	177.78	179.84	177.72
	(±6.61)	(±6.57)	(±7.33)	(±6.62)	(±6.45)	(±6.89)
	177.86	177.97	178.38	178.81	176.41	178.19

V_p, χ_t and hydrogen bonds h_p, $N_{p-1}\cdots O_{p-5}$, d_{i-4} and they are given in Figs. 4a and 4b.

The values obtained during the simulation of DP are averaged for DP1 (150 ps–200 ps) and DP2 (20 ps–130 ps) and their r.m.s. deviations are calculated. Structures at 100 ps (DP2) and 170 ps (DP1) from the simulation of DP are minimized energetically. The MD averages and r.m.s. deviations of AP2 (25 ps–55 ps and 90 ps–200 ps) and AP1 (65 ps–75 ps) of the simula-

Table 2

The distance (in Å) of the possible hydrogen bonds in the three simulations DP, AP and UP are given. The three entries for every parameter listed are the MD average, the r.m.s. deviation and the value corresponding to the MD minimized structure, respectively

Hydrogen bond distance	DP1	DP2	AP1	AP2	UP1	UP2
$N_{p-2}\cdots O_{p-6}$	2.843	2.903	3.186	2.848	3.229	2.594
	(±0.108)	(±0.187)	(±0.337)	(±0.125)	(±0.394)	(±0.260)
	2.793	2.820	3.362	2.782	3.416	3.447
$N_{p-3}\cdots O_{p-6}$	3.279	3.305	3.751	3.255	3.416	3.447
	(±0.236)	(±0.245)	(±0.384)	(±0.240)	(±0.313)	(±0.309)
	3.282	3.308	3.653	3.282	3.370	3.482
$N_{p-4}\cdots O_{p-6}$	3.448	3.455	3.538	3.439	3.568	3.552
	(±0.181)	(±0.199)	(±0.255)	(±0.194)	(±0.203)	(±0.227)
	3.459	3.464	3.438	3.463	3.590	3.659
$N_{p-1}\cdots O_{p-5}$	2.904	3.626	4.769	2.933	4.938	5.793
	(±0.134)	(±0.385)	(±0.567)	(±0.179)	(±0.467)	(±0.294)
	2.853	3.442	5.355	2.886	4.640	5.534
$N_{p-2}\cdots O_{p-5}$	3.195	3.378	5.103	3.211	2.988	3.133
	(±0.195)	(±0.350)	(±0.406)	(±0.237)	(±0.268)	(±0.293)
	3.187	3.212	5.474	3.083	2.815	2.814
$N_{p-3}\cdots O_{p-5}$	3.369	3.488	3.659	3.378	3.356	3.460
	(±0.175)	(±0.224)	(±0.222)	(±0.232)	(±0.217)	(±0.227)
	3.319	3.437	3.704	3.231	3.280	3.287
$N_{p-1}\cdots O_{p-4}$	3.819	3.403	5.965	4.105	6.031	6.004
	(±0.492)	(±0.363)	(±0.466)	(±0.541)	(±0.287)	(±0.256)
	4.231	3.334	6.289	4.531	5.998	6.047
$N_{p-2}\cdots O_{p-4}$	3.641	3.535	4.749	3.786	3.272	3.405
	(±0.281)	(±0.250)	(±0.242)	(±0.320)	(±0.286)	(±0.236)
	3.875	3.522	4.899	4.048	3.251	3.305
$N_{p+1}\cdots O_{p-3}$	4.137	6.762	2.940	3.778	6.724	6.398
	(±0.482)	(±0.724)	(±0.180)	(±0.617)	(±0.541)	(±0.310)
	3.543	6.513	2.840	2.920	6.081	6.190
$N_{p-1}\cdots O_{p-3}$	3.598	2.944	3.462	3.574	3.180	2.781
	(±0.213)	(±0.231)	(±0.187)	(±0.242)	(±0.418)	(±0.116)
	3.520	2.831	3.451	3.351	3.275	2.720
$N_{p+2}\cdots O_{p-2}$	2.840	3.186	2.886	2.848	2.941	2.908
	(±0.098)	(±0.418)	(±0.148)	(0.118)	(±0.193)	(±0.150)
	2.792	2.866	2.812	2.773	2.853	2.831
$N_{p+1}\cdots O_{p-2}$	3.082	3.002	3.337	3.205	3.026	3.065
	(±0.225)	(±0.243)	(±0.226)	(±0.236)	(±0.298)	(±0.241)
	3.172	3.145	3.312	3.229	2.787	3.122
$N_{p+3}\cdots O_{p-1}$	2.916	2.879	2.895	2.927	2.884	2.874
	(±0.149)	(±0.144)	(±0.146)	(±0.170)	(±0.135)	(±0.129)
	2.856	2.811	2.811	2.854	2.806	2.812
$N_{p+2}\cdots O_{p-1}$	3.344	3.217	3.198	3.261	3.311	3.327
	(±0.227)	(±0.242)	(±0.247)	(±0.251)	(±0.238)	(±0.231)
	3.311	3.267	3.126	3.101	3.326	3.342

tion of AP and UP2 (30 ps–70 ps and 120 ps–200 ps) and UP1 (80 ps–100 ps) of UP simulation are also calculated. The structures chosen for energy minimization from the simulation of AP are those at 70 ps (AP1) and 150 ps (AP2) and the structures chosen from UP are those at 90 ps (UP1) and 150 ps (UP2). The results obtained are compared and presented in Tables 1, 2 and 3. Table 1 gives the backbone dihedral angles, ϕ, ψ and ω obtained for the three simulations and their MD minimized structures. The distances of the possible hydrogen bonds in the three systems are calculated and presented in Table 2. Table 3 gives the results pertaining to the constraint and bend related parameters for the three systems.

The analysis indicates that the structure DP1 is close to that of normal proline containing α-helix. The characteristic features [11] namely, the MD average, the hydrogen bond h_p ($\simeq 3.5$) and the virtual torsion angle ν_p ($\simeq 61.0°$) are slightly larger than that of the normal α-helix. Also, ϕ_{p-1}, ψ_{p-1} values are close to the goniometric

Table 3

The constraint parameters and the bend related parameters (in degrees) in the three simulations DP, AP and UP are given. The three entries for every parameter listed are the MD average, the r.m.s. deviation and the value corresponding to the MD minimized structure, respectively. The energy of the minimized structures are also listed

	DP1	DP2	AP1	AP2	UP1	UP2
Constraint parameter						
$O_i^{\gamma} \cdots O_{i-4}$	2.778	4.995	2.791	2.815	2.781	2.778
	(±0.111)	(±0.545)	(±0.150)	(±0.154)	(±0.118)	(±0.112)
	2.768	4.940	2.752	2.752	2.752	2.759
$O_i^{\gamma} \cdots O_{i-3}$	4.426	2.852	4.193	4.172	4.225	4.209
	(±0.686)	(±0.306)	(±0.354)	(±0.326)	(±0.309)	(±0.296)
	5.031	2.750	4.153	4.084	4.177	4.118
C^{α}–C^{β}–C^{γ}–O^{γ}	−56.69	−17.49	−51.99	−51.24	−53.47	−53.18
	(±10.85)	(±21.75)	(±8.80)	(±8.59)	(±8.24)	(±8.58)
	−54.42	+0.72	−55.38	−54.53	−56.31	−54.60
Virtual torsion angle						
V_{p-2}	43.88	47.72	−1.71	41.93	52.57	47.99
	(±4.87)	(±5.96)	(±12.03)	(±6.13)	(±8.89)	(±7.16)
	40.22	46.56	−11.68	36.41	48.25	49.45
V_{p-1}	46.98	53.99	52.01	47.42	−132.56	−171.08
	(±4.90)	(±7.58)	(±7.93)	(±7.02)	(±15.94)	(±9.06)
	48.50	54.42	53.30	54.51	−126.35	−164.93
V_p	72.51	156.84	46.60	66.18	151.94	78.12
	(±9.33)	(±24.34)	(±5.59)	(±11.04)	(±36.19)	(±8.51)
	61.96	144.11	43.70	53.58	−168.62	70.56
V_{p+1}	39.05	53.99	44.57	39.92	45.04	47.86
	(±5.35)	(±7.58)	(±4.61)	(±6.04)	(±7.75)	(±5.41)
	37.92	50.12	47.48	40.69	44.09	48.72
V_{p+2}	49.30	47.72	49.73	50.07	46.58	46.12
	(±5.36)	(±5.96)	(±4.86)	(±5.14)	(±4.84)	(±4.88)
	51.85	44.64	48.26	52.55	44.97	44.78
Kink angle	21.10	76.36	39.13	35.07	58.32	80.08
	(±16.84)	(±13.75)	(±6.94)	(±10.79)	(±10.66)	(±7.54)
	29.31	78.36	45.60	25.50	47.58	78.10
Energy (in kcal/mol)	−341.19	−337.32	−336.67	−340.79	−330.42	−332.24

helix. The kink angle is 29.3°. In DP2, h_p distance is greater than 6.5 Å. Interestingly, an $i \rightarrow i-2$ hydrogen bond ($N_{p-1} \cdots O_{p-3}$) has gained stability, which is the characteristic of bends. This bend is correlated with change in the values of ψ_{p-2} from $-49.5°$ to $+45.0°$ resulting in ν_p of 144.1° and king angle of 78.3°. It can be seen that O^{γ} of Threonine residue makes a hydrogen bond with the backbone oxygen of the $i-3$rd residue (i corresponds to threonine residue) in DP2 and with the $i-4$th residue in DP1. Further, the conformation of the threonine dihedral angle (χ_1)

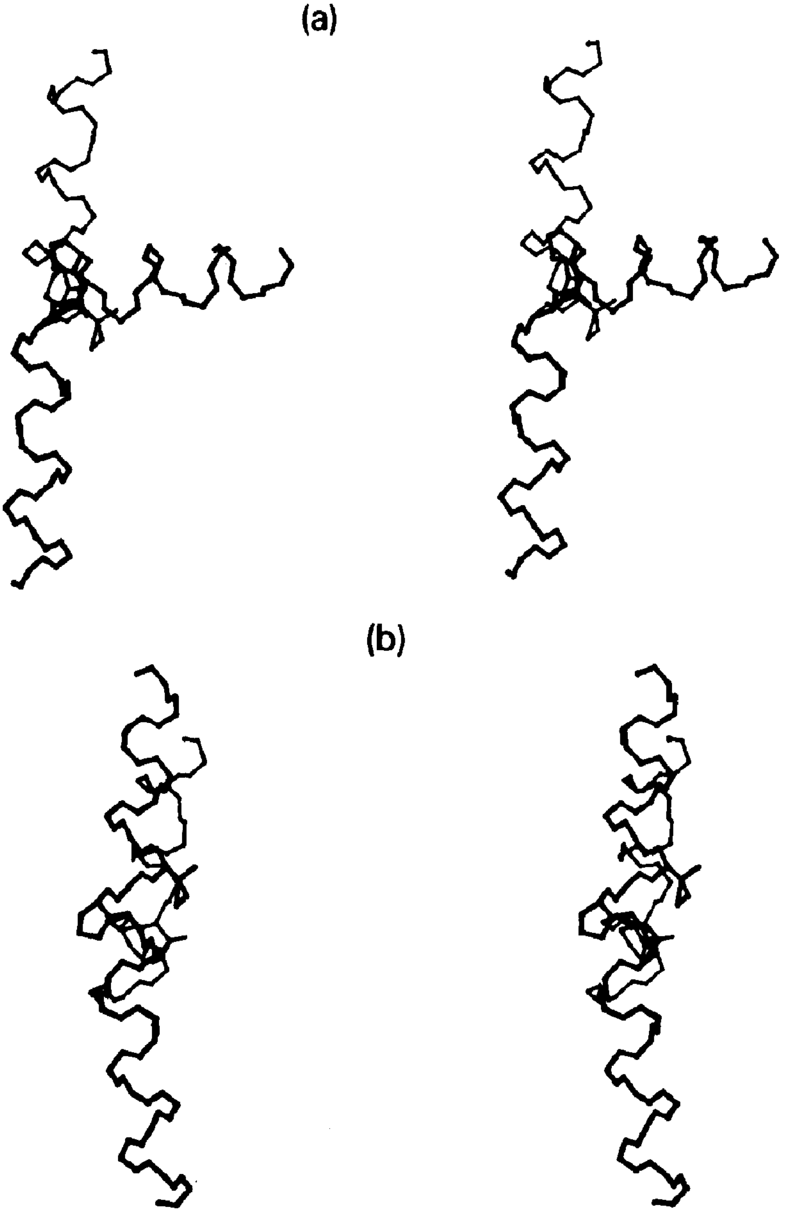

Fig. 5. A plot of the backbone atoms along with proline and threonine sidechain atoms of the superposed minimized structures of (a) DP1 and DP2 (b) AP1 and AP2, and (c) UP1 and UP2 regions.

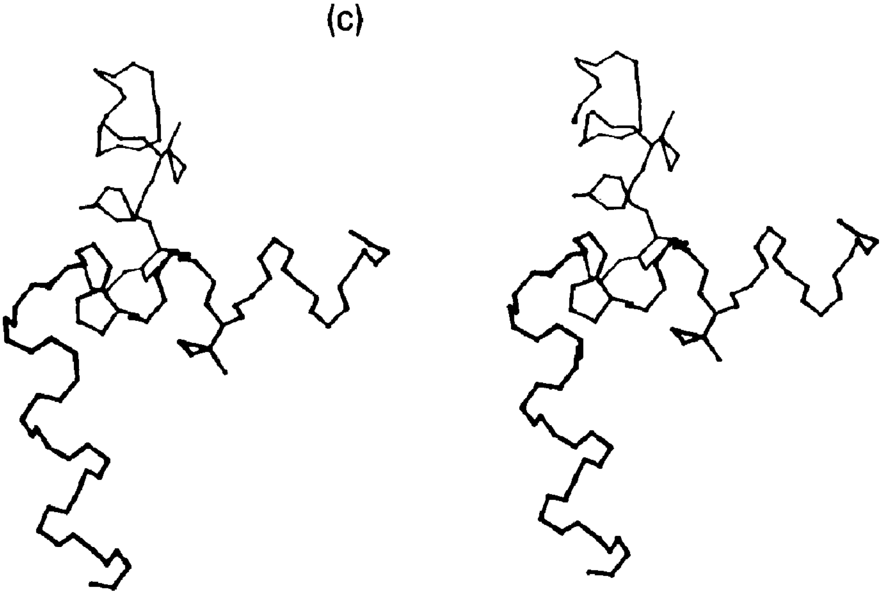

Fig. 5 continued.

in the two structures DP1 and DP2 is −54° and 0°, respectively (Table 3 and Fig. 2a). Thus, when a threonine residue is just below proline, two conformations can be accessed: a kinked helix (DP1) and a highly bent structure (DP2). This can be clearly noticed from the stereo plot of the two superposed structures, DP1 and DP2 given in Fig. 5a.

The two structures AP1 and AP2 which are accessed during the simulation of AP are given after superposition in Fig. 5b. AP2 is the structure which has been accessed for major portion of the 200 ps simulation. AP2 has the characteristics of a normal proline containing α-helix. AP1 is a bent structure. However, it is different from DP2. The kink angle of AP1 is 45.6° and the bend introduced is at p − 2nd and p − 3rd residues ('p' corresponds to the proline residue). This is evident from the comparison of hydrogen bonds and virtual torsion angles between AP1 and other structures like AP2, DP1 and DP2. The backbone hydrogen bonds involving N_{p-1} and N_{p-2} are weakened. Interestingly, this is the only structure of Proline containing helix where the hydrogen bond h_p is retained as a good hydrogen bond. The value of V_{p-2} (−12°) has significantly deviated from the normal α-helical value. At the bend, the dihedral angle ϕ_{p-2} (−125°) has taken the value of an extended structure. Thus, a constraint due to threonine-backbone interaction across the proline residue is effective in creating a structure bent below proline. However, the structure AP2 corresponding to the normal proline containing α-helix is energetically more stable and is accessed more frequently during MD simulation.

The simulation of UP has resulted in two bent structures UP1 and UP2, with UP2 being accessed for most of the time. In UP2, apart from complete disruption of the hydrogen bond h_p, $N_{p-1} \cdots O_{p-5}$ is also disrupted. It is interesting to note that $i \rightarrow i-2$ type of hydrogen bond is gained between $N_{p-1} \cdots O_{p-3}$, similar to the structure DP2. The kink angle is 78.1° and the virtual torsion angle V_{p-1} has assumed a value of −165°. The values of ψ_{p-3} (−18°) and ϕ_{p-2} (69°) have deviated from α-helical values. The structure UP1 also has lost the hydrogen bond $N_{p-1} \cdots O_{p-5}$ apart from h_p. UP1 has a king angle of 47.5° and V_p and V_{p-1} have deviated from α-helical values. The two structures are plotted in Fig. 5c. Thus, these studies on DP, AP and UP show that the application of threonine-backbone hydrogen bond constraints can result in drastic structural transitions.

The above systems have been studied in isolation. However, in the real situation, the threonine residue can interact with other groups in the environment. An interesting example is the helix C of bacteriorhodopsin (BR) where threonine 90 is just below proline. It is found to have interaction with the backbone carbonyl oxygen (O_{i-4}) and with Asp 115 of helix D [26]. Our MD studies on this structure of BR [manuscript in preparation] show that helix C retains the structure close to DP1 during the 16 ps simulation. Asp 115 is known to be involved in the proton pumping action of BR [26]. Hence either its state of protonation or its location with respect to some important groups may change during the photocycle. It is tempting to speculate that a change in Asp 115–Thr 90 interaction during the photocycle can lead to a conformational change in helix C, which thereby can lead to a large scale structural change in BR during the photocycle.

4. Summary

Recently it has been well recognized that proline introduces a bend of about 20°–30° in the α-helix [7,11,14] and a possible role of tight packing in globular proteins has been assigned [10]. Proline residues also occur in greater proportion in the membrane transport proteins than in non-transport proteins, although the significance is yet to be established. Our previous studies [11–14] showed that there is flexibility in proline containing helices. Hence its shape can be adjusted at various phases of activity depending on the process. Further, interesting results have emerged from the present studies on the effect of constraints on the structure of proline containing helices. In the present study a threonine residue has been introduced at different positions near the proline residue. In the absence of other interactions, the threonine residue forms a hydrogen bond with the back bone carbonyl oxygen. Different well defined structures are obtained during the MD simulation depending on the location of threonine. When the threonine-back bone hydrogen bond is just below the proline, the molecule can access two conformations—one being very close to the α-helix with a proline in the middle and the other assuming an extended conformation in the Proline region leading to a clear bend in the structure. The two structures are controlled by $O^{\gamma} \cdots O_{i-4}$ (d_{i-4}) and $O^{\gamma} \cdots O_{i-3}$ (d_{i-3}) threonine-backbone hydrogen bonds respectively. Thus, two structures which are topologically distinct can exist in equilibrium when a threonine residue is just below proline in an α-helix. When the threonine residue is four residues above proline, the $O^{\gamma} \cdots O_{i-4}$ (d_{i-4}) hydrogen bond can exist just above the proline. In this case, the structure close to α-helix is clearly disrupted and the helix is broken into two parts at the proline region, leading to a bent structure. Although another structure is accessed during the simulation for a short period, it is also a bent structure in comparison with an unconstrained helix with proline. A threonine residue when present at the first or second C^{α} above the proline leads to $O^{\gamma} \cdots O_{i-4}$ hydrogen bond across the proline. This type of constraint leads to an almost straight helix with very small kink similar to the structure of proline containing α-helix without any other constraint. A highly bent structure is also accessed for a short time during the simulation in which the bend occurs before the proline residue.

Thus a variety of well characterized bent structures are identified by molecular dynamics simulations by introducing constraints in the form of Threonine residue at different parts of the helix. Some of the structures and structural transitions may be important in the natural systems.

Acknowledgements

This work was partially supported by the Council of Scientific and Industrial Research scheme No. 09/0326/90-EMR-II. I wish to thank Mr. R. Sankararamakrishnan for useful discussions.

References

1 M.W. MacArthur and J.M. Thornton, J. Mol. Biol. 218 (1991) 397.

2 C.B. Anfinsen and H.A. Scheraga, Adv. Prot. Chem. 29 (1975) 205.

3 B. Robson and E. Suzuki, J. Mol. Biol. 107 (1976) 327.

4 P.Y. Chou and G.D. Fasman, Biochemistry 13 (1974) 211.

5 P.Y. Chou and G.D. Fasman, J. Mol. Biol. 115 (1977) 135.

6 G.D. Rose, L.M. Gierasch and J.A. Smith, Adv. Prot. Chem. 37 (1985) 1.

7 D.J. Barlow and J.M. Thornton, J. Mol. Biol. 201 (1988) 601.

8 J.S. Richardson and D.C. Richardson, Science 240 (1988) 1648.

9 C.J. Brandl and C.M. Deber, Proc. Natl. Acad. Sci. USA 83 (1986) 917.

10 D.N. Woolfson and D.H. Williams, FEBS Lett. 277 (1990) 185.

11 R. Sankararamakrishnan and S. Vishveshwara, Biopolymers 30 (1990) 287.

12 R. Sankararamakrishnan and S. Vishveshwara, Biophys. Chem. 40 (1991) 97.

13 R. Sankararamakrishnan and S. Vishveshwara, Int. J. Pept. Prot. Res. 39 (1992) 356.

14 R. Sankararamakrishnan and S. Vishveshwara, Prot. Struct. Function Genet., (1992) (in press).

15 R.H. Yun, A. Anderson and J. Hermans, Prot. Struct. Function Genet. 10 (1991) 219.

16 C.E. Dempsey, Biochemistry 31 (1992) 4705.

17 R. Sankararamakrishnan and S. Vishveshwara, J. Biomol. Struct. Dyn. 9 (1992) 1073.

18 P. Weiner and P.A. Kollman, J. Comp. Chem. 2 (1981) 287.

19 P.K. Weiner, U.C. Singh, P.A. Kollman, J. Caldwell and D.A. Case, A Molecular mechanics and dynamics program —AMBER (University of California, San Francisco, CA).

20 S.J. Weiner, P.A. Kollman, D.A. Case, U.C. Singh, C. Ghio, G. Alagona, S. Profeta Jr. and P. Weiner, J. Am. Chem. Soc. 106 (1984) 765.

21 S.J. Weiner, P.A. Kollman, D.J. Nguyen and D.A. Case, J. Comp. Chem. 7 (1986) 230.

22 K.C. Chou, G. Nemethy and H.A. Scheraga J. Am. Chem. Soc. 106 (1984) 3161.

23 S. Arnott and S.D. Dover, J. Mol. Biol. 30 (1967) 209.

24 L.G. Presta and G.D. Rose, Science 240 (1988) 240.

25 C. Ramakrishnan and K.V. Soman, Int. J. Pept. Prot. Res. 20 (1982) 218.

26 R. Henderson, J.M. Baldwin, T.A. Zemlin, E. Beckmann and K.H. Downing, J. Mol. Biol. 213 (1990) 899.